Model Predictive Control for High-speed Train with Automatic Trajectory Configuration and Tractive Force Optimization

Yonghua Zhou[1]**, Xun Yang**[1]**, Chao Mi**[1]

Abstract: High-speed train transportation is organized in a way of globally centralized planning and locally autonomous adjustment with the real-time known positions, speeds and other state information of trains. The hierarchical integration architecture composed of top, middle and bottom levels is proposed based on model predictive control (MPC) for the real-time scheduling and control. The middle-level trajectory configuration and tractive force setpoints play a critical role in fulfilling the top-level scheduling commands and guaranteeing the controllability of bottom-level train operations. In the middle-level MPC-based train operation planning, the continuous cellular automaton model of train movements is proposed to dynamically configure the train operation positions and speeds at appointed time, which synthetically considers the scheduling strategies from the top layer, and the tempo-spatial constraints and operation statuses at the bottom level. The macroscopic dynamic model of a train predicts the trajectories under the candidate control sequences. Through Levenberg-Marquardt optimization, the feasible tractive forces and updated trajectories are attained under the power constraints of electric machines. Numerical results have demonstrated the effectiveness of proposed control planning technique. This paper reveals the utilities of different-level models of train movements for the accomplishment of railway network operation optimization and the guaranty of individual train operation safety. It also provides a solution to automatic trajectory configuration in the automatic train protection (ATP) and operation (ATO) systems.

Keywords: train modeling, cellular automata, model predictive control, automatic train protection, automatic train operation.

---

[1] School of Electronic and Information Engineering, Beijing Jiaotong University.

1   Introduction

The construction of high-speed railway network has posed more rigorous requirements on train operation safety. One efficient measure to improve the train operation safety is to dynamically configure the proper train movement trajectories in the future such that the safety constraints are satisfied and the moderate traction and braking strategies will be implemented. The planned trajectories of a train should be constantly updated with the displacements of its preceding adjacent one. In addition, they should be enforceable under the power constraints when the loads and the resistances of the train vary. This paper attempts to address the problems of automatic trajectory configuration utilizing the train movement high-level model and of tractive force optimization through the principle of model predictive control (MPC) [Camacho and Bordons (1995)].

The application of advanced control technology to the train can be traced back to 1980s, at which time the optimal control [Gruber and Bayoumi (1982)] and fuzzy control [Yasunobu, Miyamoto, and Ihara (1983)] were explored. Afterwards, the energy-efficient train control was extensively investigated [Cheng and Howlett (1992); Howlett and Pudney (1995); Khmelnitsky (2000); Liu and Golovitcher (2003); Howlett, Pudney, and Vu (2009)]. The fuzzy optimal control [Jia and Zhang (1993)] and H_2/H_∞ control [Yang and Sun (2001)] were developed to deal with the multi-objective control of trains. The heavy-haul train control was also extensively studied through linear quadratic regulator (LQR) [Chou and Xia (2007)], measured output feedback control [Zhuan and Xia (2008)], fault-tolerant control [Zhuan and Xia (2010)], etc. With the rapid development of wireless communication technology, it has been attempted to be applied to the high-speed train control system. There exists a little literature dealing with the high-speed train automatic operation utilizing the methods such as parallel control and management [Ning, et al (2011)], adaptive control [Song, et al (2011)], fuzzy control [Dong, et al (2013)], iterative learning control [Wang, Hou, and Li (2008)], and model predictive control [Zhou and Wang (2011)], etc.

The very important aspect of train control is to satisfy the power constraints during the total train movement process. The general control law of driving electric machines is that at the low speeds, the constant torque control is implemented, and after a certain speed, the constant power control is enforced. When the train arrives at a certain speed, the remained acceleration or driving force should be subject to the power constraint. The bigger the speed is, the smaller the remained acceleration is. If the train movement trajectories are implementable in view of the output power, the train operation safety can be guaranteed. Or, the train can not stop at a specified point and the accident of train crash might happen in the high-speed railway network.

The train movement model based on the principle of cellular automata [Nagel and Schreckenberg (1992); Chowdhury, Santen, and Schadschneider (2000)] explicitly describes the transition constraints and the relationships of speed updates with accelerations and decelerations, which provides a simple measure to plan the train movements at the macroscopic and mesoscopic levels. The cellular automaton (CA) models for railway traffic were proposed to replicate the realistic train movements [Li, Gao, and Ning (2005); Ning, Li, and Gao (2005)]. Several improved models were developed to describe the moving- or moving-like block system [Xun, Ning, and Li (2007); Zhou, Gao and Li (2006)], to capture the driver reaction [Tang and Li (2007)], to consider the speed limits in the fixed-block systems [Fu, Gao, and Li (2007)], and to describe the train movements at station [Xun, Ning, and Li (2009)]. A generalized train movement model was explored to describe the train movements under scheduling and control with various tempo-spatial constraints [Zhou and Mi (2012)]. It models the feedback driving behavior [Zhou, Mi and Yang (2012)], and establishes the connection between the top-level scheduling and the bottom-level control.

The limitation of CA model is that the acceleration and deceleration should be integer. However, in practice the acceleration and deceleration for the railway traffic are generally less than 1. In order to utilize the train movement CA model, the complex transformation will be involved to make the acceleration and deceleration be integer through properly defining the length of a cell. The train movement model with speed limits was presented for the railway network, which directly employs the practical acceleration and deceleration [Lu, Dessouky and Leachman (2004)]. This paper will extend the generalized train movement model to the case directly utilizing any variable acceleration and deceleration. We will apply the extended model to configure the train movement trajectories with the feasible accelerations and decelerations from practical data. The remained problem is to find the control sequences (decision variables) such that the predicted movement trajectories approach the configured ones. It is actually a problem of nonlinear algebraic equation F(x)=0 [Liu and Atluri (2011); Liu, Dai, and Atluri (2011a, 2011b); Liu and Atluri (2012)]. In this paper, we will employ the basic Levenberg-Marquardt optimization technique to solve this problem. The tractive force constraints will be taken into account during the optimization process. The procedure is implemented in the rolling horizon such that the planning of positions, speeds and tractive forces can be adjusted according to the real-time feedback information. Consequently, the bottom-level train movement control can be executed according to the middle-level setpoints considering the requirements of top-level scheduling and the controllability of bottom-level train operation.

The rest of this paper is organized as follows. In section 2, the hierarchical in-

tegration architecture of real-time train scheduling and control based on MPC is outlined. Section 3 develops the extended train movement model and the trajectory configuration approach. Section 4 presents the planning approach of train movements based on MPC with automatic trajectory configuration at the middle level. The numerical results are demonstrated and elucidated in section 5. Finally, the conclusions are drawn in section 6.

2   Integration architecture of train scheduling and control based on MPC

Train scheduling and control are the two mutually dependent elements for train operation. Under the slow- and medium-speed railway transportation infrastructure, scheduling and control are not so frequently integrated because the train operation states can not be immediately transmitted to the ground commanding center. In the high-speed railway network, the train positions, speeds and other state information can be reported to the ground commanding center in a real-time manner, which makes it possible to accomplish the timely scheduling. Consequently, the train control systems can obtain the real-time updated scheduling commands which facilitate the operation safety and efficiency.

MPC is a feedback- and prediction-based optimization technique of control strategies, which can play a significant role in improving the operation safety of high-speed train because the potential danger can be predicted and prevented beforehand. Based on the MPC technique, Fig. 1 outlines the hierarchical integration framework of real-time train scheduling and control. It includes three levels, i.e. macroscopic (top), mesoscopic (middle) and microscopic layers. At the macroscopic level, the optimized scheduling strategies are engendered in view of the operation optimization of total railway network, which specify where the train should locate at appointed time. They are generalized movement authority which describes both how long and how fast the train can move. At the mesoscopic level, the detailed individual train operation plan is produced, which fulfills the top-level scheduling strategies and justifies the control feasibilities. At the microscopic level, each car of a train is controlled such that the commands from the mesoscopic level are carried out. There exist various control strategies for the car control, among which MPC is an alternative way depicted with dotted lines in Fig. 1. The objective of the top layer is accomplished at the ground commanding center including the equipment such as radio block center (RBC) and centralized traffic control (CTC), and the one of the bottom layer is implemented at the cars of the train. The goal of the mesoscopic layer can be executed either at the ground commanding center or at the vital computer mounted in the locomotive of the train.
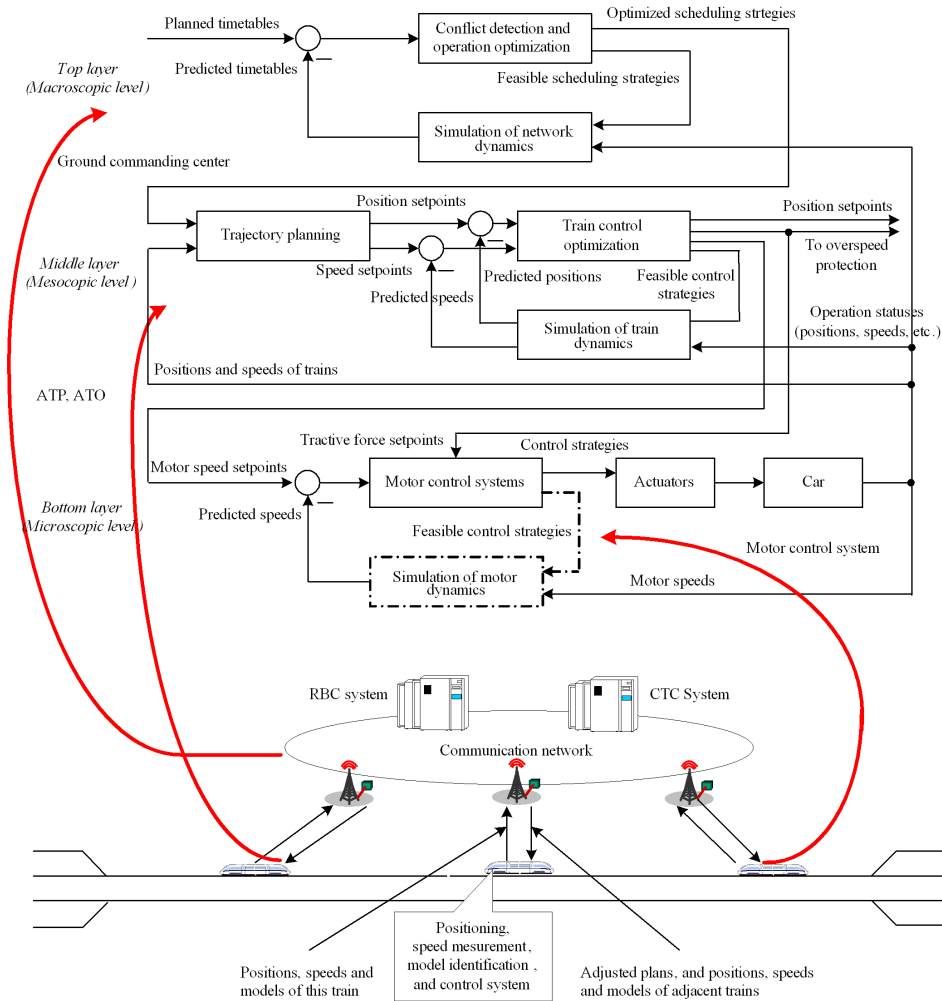
Figure 1: The hierarchical integration architecture of real-time train scheduling and control

3 Automatic trajectory configuration utilizing train movement model

3.1 Train movement high-level modeling

The high-level model is generally oriented towards the analysis and decision at the macroscopic and mesoscopic layers of complex systems. In this subsection, we will extend the train movement high-level model [Zhou and Mi (2012)] to the case with any variable accelerations and decelerations. Set the proposed train movement model in the moving-block system [Takeuchi, Goodman, and Sone (2003)] as an example to illustrate the train movement planning process at the mesoscopic level. For the fixed-block system, the planning process is similar. We first define the following notations.

x_k : the position of train on the railway line at instant kT where T is the period. T is generally omitted when specifying an instant in the description of discrete-time system.

v_k : the speed of train at instant kT.

$v_{\max}$: the maximum speed of train.

$v_{\lim}(x)$: the most restrictive speed profile related to the position x on the railway line.

a_k : the acceleration of train at instant kT.

b_k : the deceleration of train at instant kT.

v_t : the required speed of train at target point.

d_t : the distance to the instantaneous target point where the speed of train is v_t.

d_m : the distance to the target point where the speed of train is 0.

d_b : the braking distance when the speed of train decelerates from v_k to v_t.

d_r : the braking reference distance which is equal to $d_b + v_k$.

The extended train movement model is described as follows.

(1) Speed update

```
if vk > vlim(xk), vk+1 = max(vk − bk, 0)
elseif vk = vlim(xk) AND dt ≥ dr, vk+1 = vk
else
   if dt > dr, vk+1 = min(vk + ak, vk + dt − dr )
   elseif dt = dr, vk+1 = vk
   else
       if vk = vt ≠ 0, vk+1 = vk
       else vk+1 = min(max(vk − bk, vk − (dr − dt), vt),dm)
       end
```

    end
end

(2) Position update

$$x_{k+1} = x_k + v_{k+1}$$

In the above model, we assume that the train runs towards the instantaneous target point and all the variables are nonnegative. During the trajectory configuration process, the case that the train runs away from the target point might happen. In this case, the braking process is unconditionally initiated until the target point locates in front of the train. The positive direction of position and speed is the one from the departure station to the destination. The goal of trajectory configuration is to make the train gradually transit onto the basic braking reference curve. With regard to this purpose, the extra acceleration and deceleration constraints are complemented into the above model, compared with the generalized train movement model [Zhou and Mi (2012)]. Actually, it models the train movements with advanced ATP. If $v_k > v_{\lim}(x_k)$, according to the difference degree between v_k and $v_{\lim}(x_k)$, the corresponding deceleration b_k will be adopted for the related braking level such as the service or emergency braking.

3.2   *Train movement trajectory configuration*

In this subsection, we will use the practical data of high-speed train CRH3 to illustrate the trajectory configuration of train movements. Because of the power limits, the available tractive and braking forces are related to the train speeds as shown in Fig. 2 (a). The basic resistance generally monotonically ascends with the increase of speed. Define $F_t(v_k)$ and $F_b(v_k)$, denoting the tractive and braking forces (in absolute value) at speed v_k, respectively. $f(v_k)$ represents the basic resistance corresponding to v_k. Given the train mass m, according to Fig. 2 (a), the available acceleration and deceleration at certain speed v_k can be obtained through $a_k = (F_t(v_k) - f(v_k))/m$ and $b_k = (F_b(v_k) + f(v_k))/m$, respectively, which are depicted in Fig. 2 (b). Consequently, the acceleration and deceleration processes can be attained through $v_{k+1} = v_k + a_k T$ and $v_{k+1} = v_k - b_k T$, respectively. Fig. 2 (c) and (d) show the acceleration and deceleration limitation curves, respectively. They can be fitted utilizing the exponential curves $Av_{\max}(1 - e^{-\alpha t})$ and $Bv_{\max}(1 - e^{-\beta(T_b - t)})$ where A, B, α and β are the positive coefficients to be identified, t is the continuous time here, and T_b is the time decelerating from $v_{\max}$ to 0. The feasible acceleration and deceleration processes can be acquired through making α and β smaller. Fig. 2 (e) and (f) demonstrate the acceleration and deceleration distances, respectively. Fig. 2 (f) is a very critical curve for the trajectory

configuration through which d_b corresponding to the speed v_k is attained. Because the mass and the resistances of a train may alter during the train operation process, Fig. 2 (f) should be acquired on line. Fig. 2 (g) and (h) demonstrate the configured trajectories when the target points with speed 0 are at the positions of 10km and 60km, respectively. In Fig. 2 (f), because the target point is near, the train can not accelerate to the maximum speed $v_{max} = 350km/h$. In Fig. 2 (g), the target point is far enough to allow the train to accelerate to v_{max}.
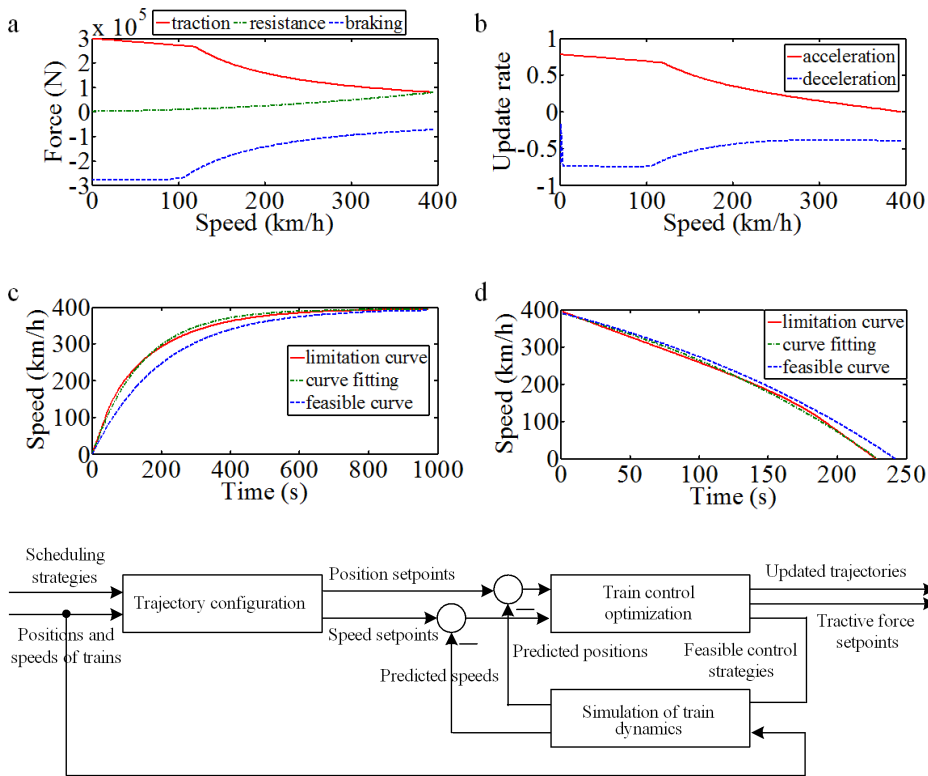

Figure 2: The curves required and engendered in automatic trajectory configuration. (a) tractive and braking forces, and basic resistance, (b) speed update rate, (c) acceleration process, (d) deceleration process, (e) acceleration distance, (f) deceleration distance, (g) configured trajectory 1, and (h) configured trajectory 2.

4 MPC for train operation planning

4.1 Basic framework

Fig. 3 describes the basic framework of train operation planning. MPC is utilized to further justify the control feasibility under the power constraints and update the position and speed profiles in the rolling prediction horizon. The trajectory configuration employs the proposed train movement model considering the scheduling strategies and the real-time positions and speeds of trains [Zhou and Mi (2012)]. MPC engenders the adjusted position and speed trajectories in case of the variations of the train mass and resistances under the control of optimized tractive forces.
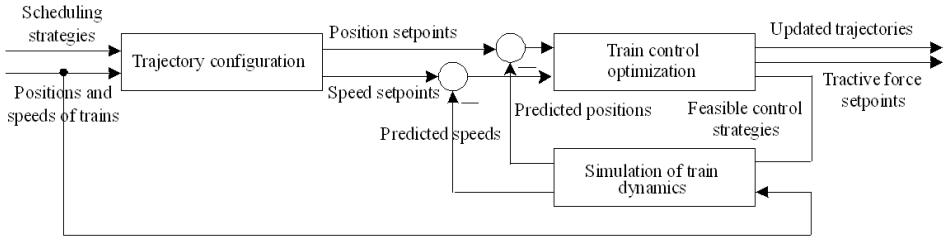

Figure 3: Basic framework of train operation planning based on MPC with automatic trajectory configuration

4.2 Optimization model

The individual train movement can be described by the following nonlinear state-space equation:

$$\dot{x} = v \tag{1}$$

$$\dot{v} = (u - r_b(v) - r_e(x))/m \tag{2}$$

where x is the position, v is the speed and m is the mass of train. u is the tractive force. $r_b(v)$ is the resistance of running train, which is related to the speed and mass, and synthetically denoted as $r_b(v) = m(av^2 + bv + c)$. $r_e(x)$ is the extra resistance caused by the position particularities such as the slope and curve of railway line. For simplicity, $r_e(x)$ is omitted in the following discussion.

We utilize the following discrete state-space equation as the prediction model in MPC:

$$x(k+1) = x(k) + v(k+1)T \tag{3}$$

$$v(k+1) = v(k) + \frac{T}{m}u(k) - T\left(av^2(k) + bv(k) + c\right) \tag{4}$$

where the period T is generally omitted in the expression of discrete instant kT. The objective function of MPC is

$$L(k) = \frac{1}{2}\sum_{i=1}^{P}[\lambda_x\left(x_s(k+i) - x_p(k+i)\right)^2 + \lambda_v\left(v_s(k+i) - v_p(k+i)\right)^2 \\ + \lambda_u\left(u(k+i-1)\right)^2] \tag{5}$$

where $x_s(k+i)$ and $x_p(k+i)$ are the setpoints and the predictions of positions in the prediction horizon P (T is generally omitted in MPC) at instant kT, respectively. Similarly, $v_s(k+i)$ and $v_p(k+i)$ are the setpoints and the predictions of speeds in the prediction horizon P at instant kT. $u(k+i-1)$ is the control sequences in the prediction horizon P at instant kT. λ_x, λ_v and λ_u are the weighting coefficients. In Eq. 5, the control horizon M in MPC is set to be equal to the prediction horizon P.

4.3 Levenberg-Marquardt optimization

Making a simple transformation on Eq. 5, we can obtain

$$L(k) = \frac{1}{2}\mathbf{e}^{\mathbf{T}}(k)\mathbf{e}(k) \tag{6}$$

where

$$\mathbf{e}(k) = \begin{bmatrix} \mathbf{e}_1(k) \\ \mathbf{e}_2(k) \\ \mathbf{e}_3(k) \end{bmatrix} = \begin{bmatrix} \sqrt{\lambda_x}\left(\mathbf{X}_s(k) - \mathbf{X}_p(k)\right) \\ \sqrt{\lambda_v}\left(\mathbf{V}_s(k) - \mathbf{V}_p(k)\right) \\ \sqrt{\lambda_u}\mathbf{u}(k) \end{bmatrix} \tag{7}$$

$$\mathbf{X}_s(k) = [x_s(k+1)x_s(k+2)\cdots x_s(k+P)]^{\mathbf{T}} \tag{8}$$

$$\mathbf{X}_p(k) = [x_p(k+1)x_p(k+2)\cdots x_p(k+P)]^{\mathbf{T}} \tag{9}$$

$$\mathbf{V}_s(k) = [v_s(k+1)v_s(k+2)\cdots v_s(k+P)]^{\mathbf{T}} \tag{10}$$

$$\mathbf{V}_p(k) = [v_p(k+1)v_p(k+2)\cdots v_p(k+P)]^{\mathbf{T}} \tag{11}$$

$$\mathbf{u}(k) = [u(k)u(k+1)\cdots u(k+P-1)]^{\mathbf{T}}. \tag{12}$$

According to the Levenberg-Marquardt (L-M) optimization, the updating rate of input $\mathbf{u}(k)$ is

$$\Delta\mathbf{u}(k) = -(\mathbf{J}^{\mathbf{T}}\mathbf{J} + \mu\mathbf{I})^{-1}\mathbf{J}^{\mathbf{T}}\mathbf{e} \tag{13}$$

where μ is the adjustable parameter iteratively increased or decreased at the rate of r_μ, I is the identity matrix, and J is Jacobian matrix which is calculated by

$$\mathbf{J} = \frac{\partial \mathbf{e}}{\partial \mathbf{u^T}} = \begin{bmatrix} \frac{\partial \mathbf{e_1}}{\partial \mathbf{u^T}} \\ \frac{\partial \mathbf{e_2}}{\partial \mathbf{u^T}} \\ \frac{\partial \mathbf{e_3}}{\partial \mathbf{u^T}} \end{bmatrix} = \begin{bmatrix} \mathbf{J_1} \\ \mathbf{J_2} \\ \mathbf{J_3} \end{bmatrix}. \tag{14}$$

Substituting Eqs. 7-12 and 14 into Eq. 13 yields

$$\Delta \mathbf{u}(k) = - \left(\lambda_x \mathbf{J_1^T J_1} + \lambda_v \mathbf{J_2^T J_2} + (\lambda_u + \mu)\mathbf{I} \right)^{-1} \left(\lambda_x \mathbf{J_1^T e_1} + \lambda_v \mathbf{J_2^T e_2} + \lambda_u \mathbf{u} \right). \tag{15}$$

$\mathbf{J_1}$ and $\mathbf{J_2}$ are, respectively, calculated by

$$\mathbf{J_1} = \frac{\partial \mathbf{e_1}}{\partial \mathbf{u^T}} = -\frac{\partial \mathbf{X}_p}{\partial \mathbf{u^T}} = -(\gamma_{i,j})_{P \times P} \tag{16}$$

$$\mathbf{J_2} = \frac{\partial \mathbf{e_2}}{\partial \mathbf{u^T}} = -\frac{\partial \mathbf{V}_p}{\partial \mathbf{u^T}} = -(\delta_{i,j})_{P \times P} \tag{17}$$

where

$$\gamma_{i,j} = \begin{cases} \delta_{i,j} T & i = j, i = 1,...,P \\ \gamma_{i-1,j} + \delta_{i,j} T & i > j, i = 2,...,P \\ 0 & otherwise \end{cases} \tag{18}$$

$$\delta_{i,j} = \begin{cases} T/m & i = j, i = 1,...,P \\ (1 - bT - 2aT v_p(k+i-1))\delta_{i-1,j} & i > j, i = 2,...,P \\ 0 & otherwise \end{cases} . \tag{19}$$

4.4   Optimization algorithm

1) Initialize. Set the initial values for the following variables:

μ : the adjustable parameter in Eq. 13,

$\mu_{\max}$: the specified maximal value of μ,

$\mu_{\min}$: the specified minimal value of μ,

r_μ : the adjustment rate of μ,

$\mathbf{u}_{temp}(k)$: the temporary value of $\mathbf{u}(k)$,

L_{min}: the specified minimal value of $L(k)$,

L_l: the minimum value of $L(k)$ obtained in the last iterative steps,

s: the iterative step,

cycle: the specified maximal number of iterative steps.

2) Calculate setpoints $\mathbf{X}_s(k)$ and $\mathbf{V}_s(k)$ according to Section 3.

3) Set the initial input $\mathbf{u}_{temp}(k)$. Suppose the optimized control inputs in the last simulation period are $\mathbf{u}(k-1)=[u(k-1)\,u(k)\ldots u(k+P-2)]^T$, and then $\mathbf{u}_{temp}(k)=[u(k)\,u(k+1)\,\ldots\,u(k+P-2)\,u(k+P-2)]^T$.

4) Predict. Calculate $\mathbf{X}_p(k)$ and $\mathbf{V}_p(k)$ according to Eqs. 3 and 4 using $\mathbf{u}_{temp}(k)$.

5) Calculate L(k) according to Eqs. 6-12 using $\mathbf{u}_{temp}(k)$.

6) Check. If $L(k) < L_{min}$, go to step 11).

7) Update μ and $\mathbf{u}(k)$. If $L(k) < L_l$, then $\mathbf{u}(k)=\mathbf{u}_{temp}(k)$, $L_l = L(k)$, and $\mu = \mu/r_\mu$, and otherwise $\mu = r_\mu\mu$. If $\mu > \mu_{\max}$, $\mu = \mu_{\max}$. And if $\mu < \mu_{\min}$, $\mu = \mu_{\min}$.

8) Calculate the Jacobian matrix according to Eqs. 16-19.

9) Calculate $\mathbf{u}_{temp}(k)$. Calculate $\Delta\mathbf{u}(k)$ according to Eq. 15, and then $\mathbf{u}_{\mathbf{temp}}(k) = \mathbf{u}_{\mathbf{temp}}(k)+\Delta\mathbf{u}(k)$.

10) Check. $s=s+1$. If $s < cycle$, then go to step 2).

11) Output u(k) at the current instant. $u(k)=[1\,0\,\ldots\,0]\mathbf{u}(k)$.

5   Numerical results

5.1   Case I

In case I, the train departs from the position of $0km$ and stops at the position of $10km$, in which case the train can not accelerate to the maximum speed $v_{\max} = 350km/h$. The simulation period T is $1s$, the prediction horizon $P = 20$, and the simulation time is $1000s$. $\lambda_x = 0.5$, $\lambda_v = 0.5$, and $\lambda_u = 0$ in the case studies. Fig. 4 (a) demonstrates the configured trajectories in the total simulation process utilizing the proposed high-level model of train movements and considering the feedback information of train positions and speeds. They include the acceleration and deceleration processes. Fig. 4 (b) represents the optimization process within 200 optimization cycles for each simulation period. At the first simulation period, the initial values of the control sequences in the prediction horizon are set as $u(k+i) = 0, k = 1, i = 1, ..., P-1$. From Fig. 4 (b), we can learn that the objective function value $L(k)$ can be convergent to a small one within the 50 optimization cycles. At the remained simulation periods, the control sequences will be set as described in *step* 3 in Section 4.4. Hence, the initial objective function value is small at the first optimization cycle, and the total objective function values are also small for the remained 199 optimization cycles in each remained simulation period. Fig. 4 (c) is the control sequences in the prediction horizon obtained in the optimization process within 200 cycles in each simulation period. The stable control sequences can be observed in the steady-state control phase. The optimized tractive force set-
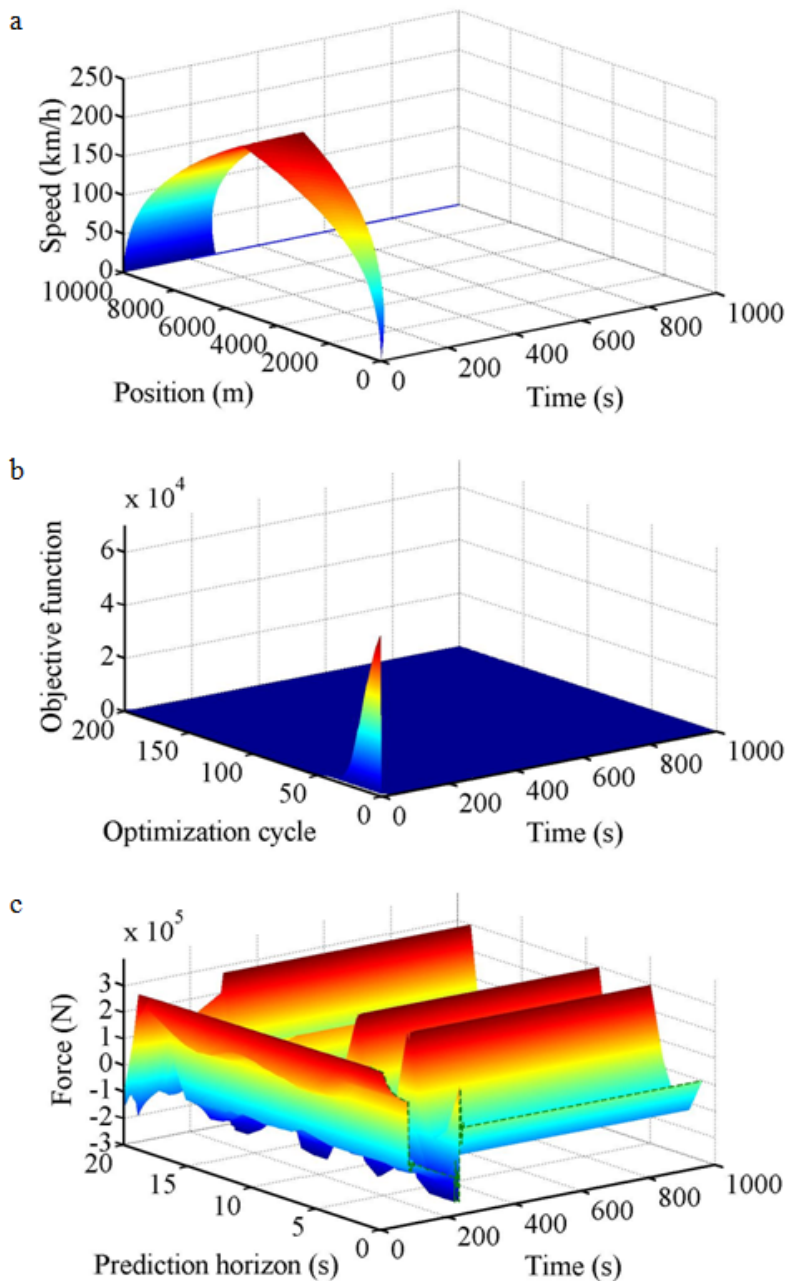
Figure 4: Optimization process of tractive force. (a) configured trajectory, (b) optimization process, and (c) tractive force.
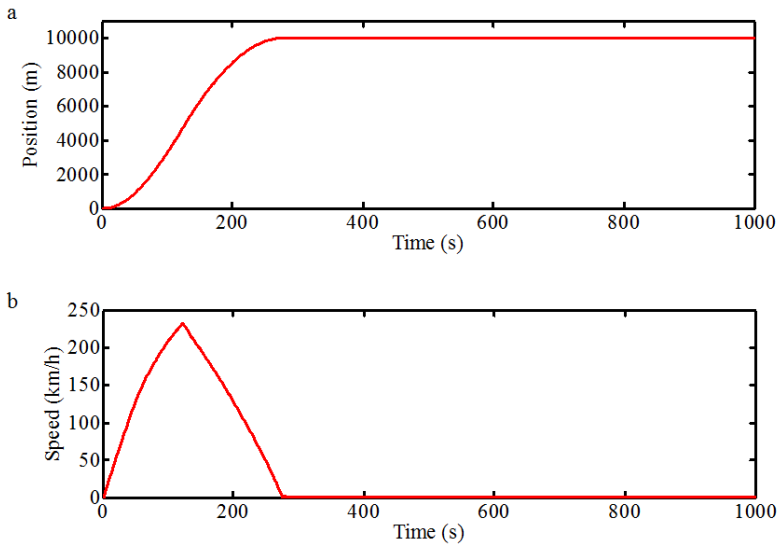
Figure 5: Updated trajectories. (a) position versus time, and (b) speed versus time.

points for the actual controllers are shown with dotted line in Fig. 4(c). Fig. 5 demonstrates the updated distance and speed curves related to time, which are the setpoints for the actual controllers and corresponding to the feasible tractive force setpoints. The speed profile is similar to the contour of Fig. 4 (a). The synthetic curve of speed versus position from Fig. 5 is the part of most restrictive speed profile $v_{\lim}(x)$ for the vital computer in the ATP system.
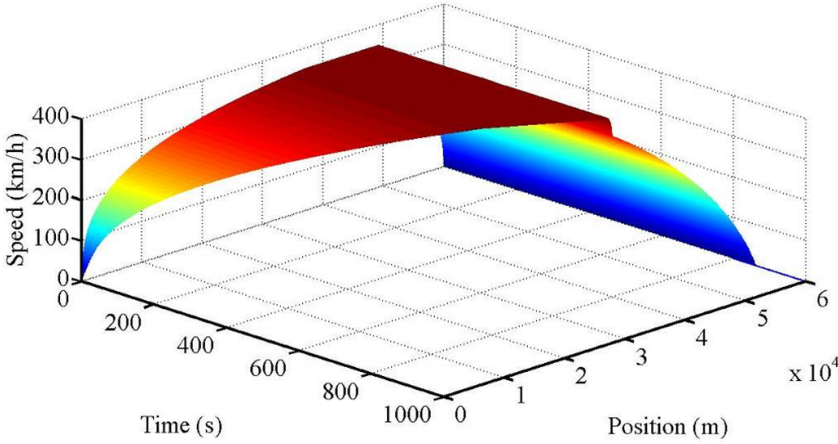
Figure 6: Configured trajectory.

5.2 Case II

In case II, the train departs from the position of $0km$ and stops at the position of $60km$, in which case the train can accelerate to $v_{max} = 350km/h$. The speed holding process can be observed in Fig. 6 and Fig. 7 (c) besides the acceleration and deceleration processes. Fig. 7 (a) demonstrates the optimized tractive forces satisfying the power constraints as shown in Fig. 2 (a). Fig. 7 (b) represents the curve of position and time. The speed profile in Fig. 7 (c) is consistent with the contour of trajectories described in Fig. 6.

5.3 Case III

In case III, two trains depart from the positions of $0km$ and $15km$, respectively, and both run towards the position of $100km$. The safe margin when two trains stop is $5km$. The maximum speed of front train is $v_1^{max} = 250km/h$, and the maximum speed of back one is $v_2^{max} = 350km/h$. The speed holding process for the front train can be observed in Fig. 8 and Fig. 9(b). However, the speeds of the back train are restrained by those of the front one, thus the back train can not accelerate to v_2^{max}, and it runs with the speed of v_1^{max} during some periods as shown in Fig. 8 and Fig. 9 (b). The distance between two trains is maintained greater than the sum of braking distance corresponding to the speed and safe margin. In the final stopping stage, the distance between two trains is the safe margin as shown in Fig. 9 (a).
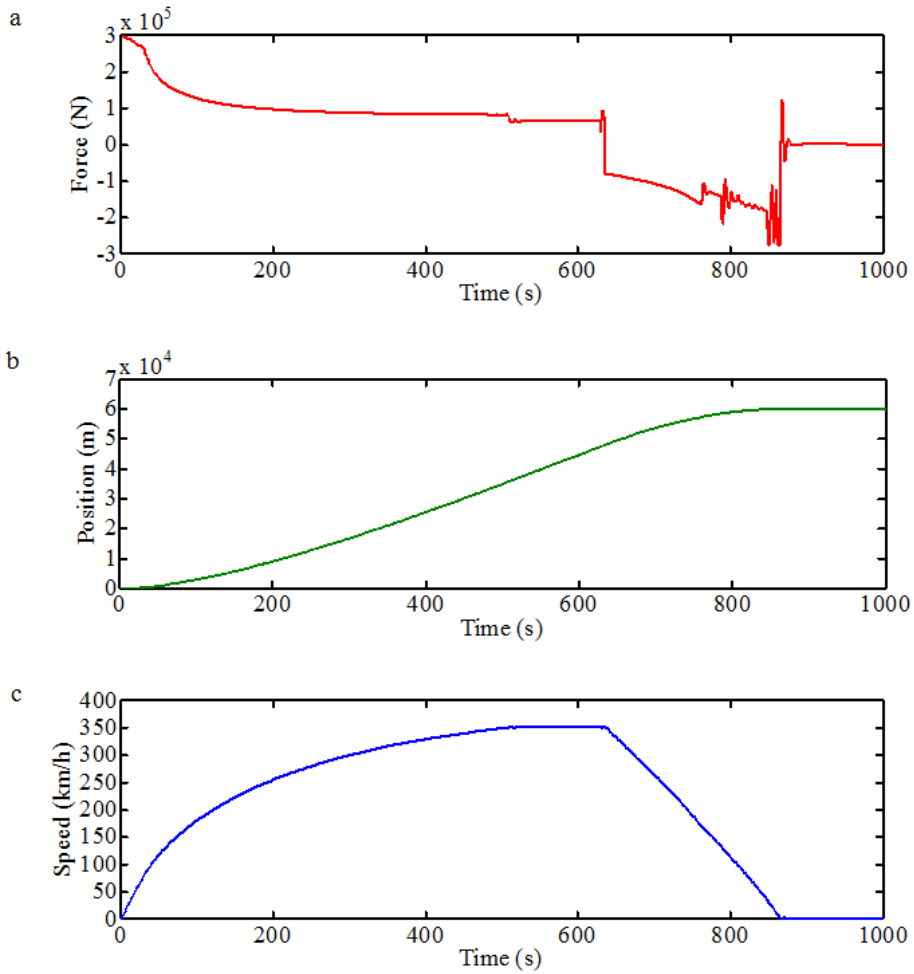
Figure 7: Optimized tractive force and updated trajectories. (a) tractive force, (b) position versus time, and (c) speed versus time.
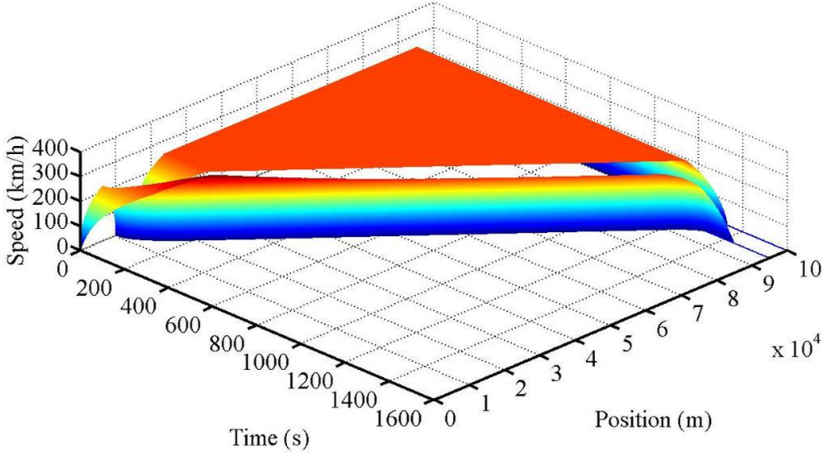
Figure 8: Configured trajectory.

Fig. 9 (b) is the part of most restrictive speed profile $v_{\text{lim}}(x)$ for the vital computer in the ATP system. The optimized tractive forces are shown in Fig. 9 (c).

5.4 Case IV

In case IV, two trains depart from the positions of $0km$ and $30km$, respectively, and both run towards the position of $100km$. The safe margin is also $5km$. In this case, both trains have the chances to accelerate to the same maximum speed $v_{\text{max}} = 350km/h$. The speed holding process for two trains can be observed in Fig. 10 and Fig. 11(b). Fig. 11 (a) utilizing the curve of position versus time depicts the following behavior of the back train with the front one. Fig. 11 (b) displays the curve of speed versus distance, a reference to produce the braking command for the vital computer in the ATP system. The piecewise smooth and optimized tractive forces are obtained as shown in Fig. 11 (c).

6 Conclusions

Automatic trajectory configuration is an important function of automatic train protection (ATP) and operation (ATO) systems. It provides a curve of speed versus position for the braking reference in case of overspeed and the driving guidance for the train operation. In this paper, we have demonstrated how the proposed train movement high-level model, providing the interfaces for the top-level scheduling commands and the dynamic target positions of the preceding adjacent train, can
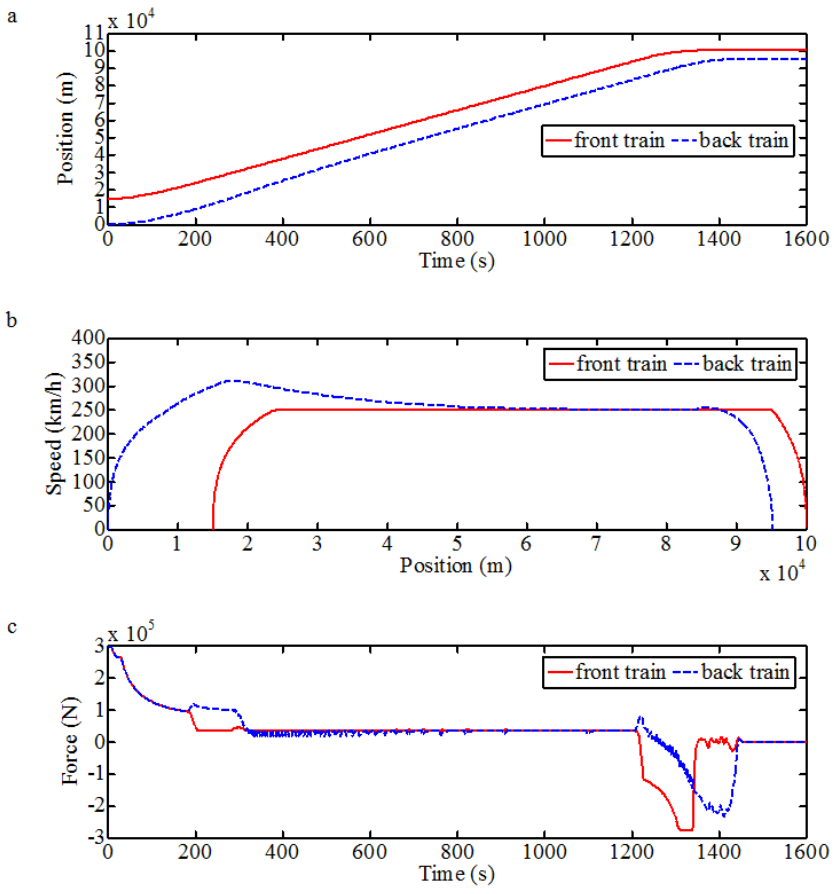
Figure 9: Train following process, updated trajectory and optimized tractive force. (a) position versus time, (b) speed versus position, and (c) tractive force.
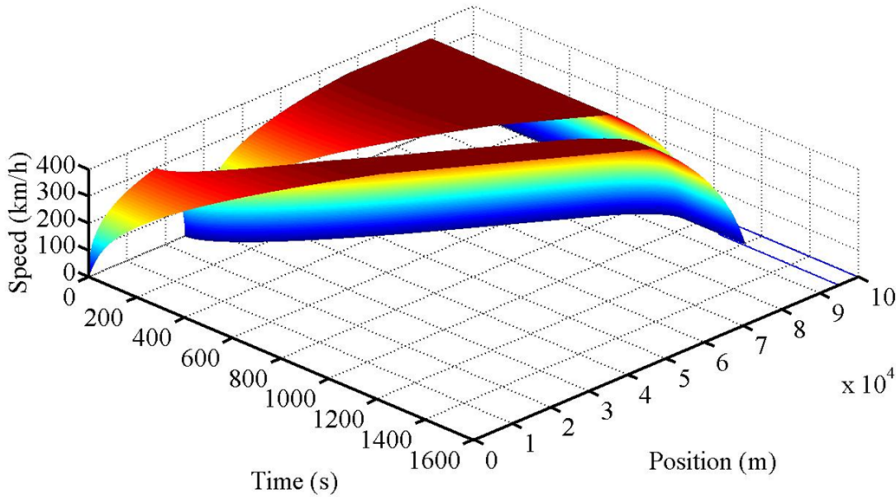
Figure 10: Configured trajectory.

be a useful tool for the trajectory configuration. Besides, the setpoints of tractive forces (proportional to the electric currents of driving machine) are also important criteria for the bottom-level car control of a train. The principle of model predictive control is employed to find out the proper tractive force sequences considering the power constraints to make the predicted trajectories approach the configured ones, during which the predicted trajectories are obtained through the macroscopic train dynamic model. Consequently, the control inputs are optimized and the updated trajectories are attained according to the real-time feedback information. Various case studies have demonstrated the validity of proposed train operation planning approach. The further work is on one hand to utilize the complex train movement model as the prediction model in MPC considering the counterforce dynamics between the cascaded cars, and on the other hand to employ the advanced optimization technique to solve the problem of nonlinear algebraic equation $F(x)=0$ [Liu and Atluri (2011); Liu, Dai, and Atluri (2011a, 2011b); Liu and Atluri (2012)] so that more accurate tractive forces can be attained.
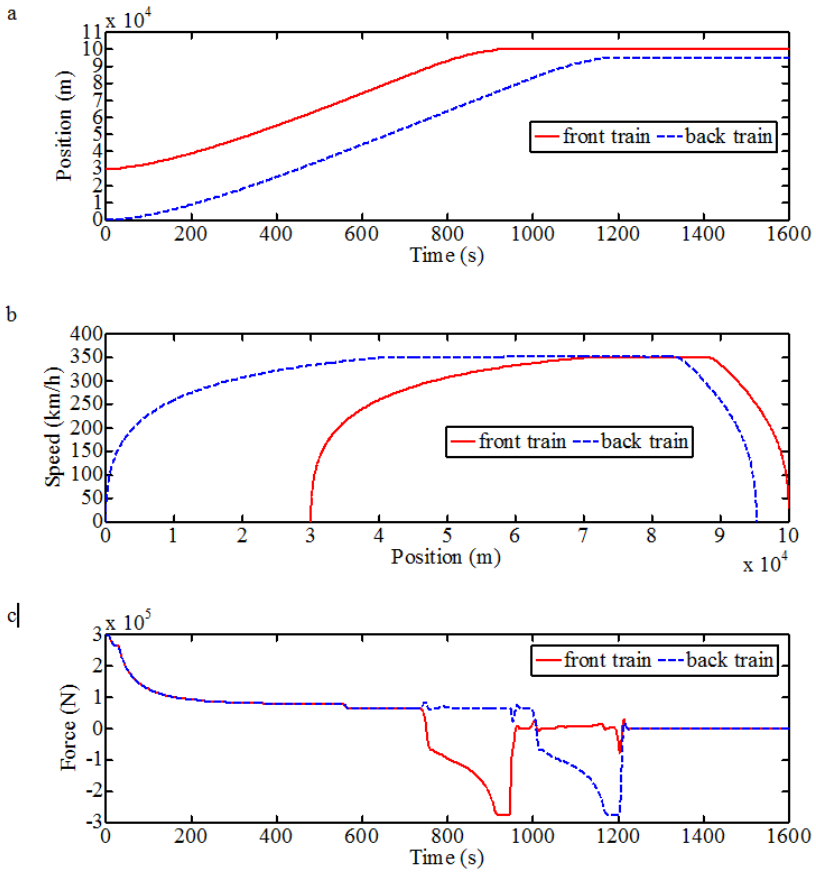
Figure 11: Train following process, updated trajectory and optimized tractive force. (a) position versus time, (b) speed versus position, and (c) tractive force.

References

Camacho, E.; Bordons, C. (1995): *Model predictive control in the process industry.* Springer Press.

Cheng, J.; Howlett, P. (1992): Application of critical velocities to the minimisation of fuel consumption in the control of trains. *Automatica*, vol. 28, pp. 165-169.

Chou, M.; Xia, X. (2007): Optimal cruise control of heavy-haul trains equipped with electronically controlled pneumatic brake systems. *Control Eng. Pract.*, vol. 15, pp. 511-519.

Chowdhury, D.; Santen, L.; Schadschneider, A. (2000): Statistical physics of vehicular traffic and some related systems. *Phys. Rep.*, vol. 329, pp. 199-329.

Dong, H.-R.; Gao, S.-G.; Ning, B.; Li, L. (2013): Extended fuzzy logic controller for high speed train. *Neural Comput. & Applic.*, vol. 22, pp. 321-328.

Fu, Y.-P.; Gao, Z.-Y.; Li, K.-P. (2007): The characteristic analysis of the traffic flow of trains in speed-limited section for fixed-block system. *Acta Phys. Sin.*, vol. 56, pp. 5165-5171.

Gruber, P.; Bayoumi, M. M. (1982): Suboptimal control strategies for multilocomotive powered trains. *IEEE Trans. Automat. Contr.*, vol. 27, pp. 536-546.

Howlett, P. G.; Pudney, P. J. (1995): *Energy-efficient Train Control.* Springer Press.

Howlett, P. G.; Pudney, P. J.; Vu, X. (2009): Local energy minimization in optimal train control. *Automatica*, vol. 45, pp. 2692-2698.

Jia, L.-M.; Zhang, X.-D. (1993): On fuzzy multiobjective optimal control. *Eng. Applic. Artif. Intell.*, vo. 6, pp. 153-164.

Khmelnitsky, E. (2000): On an optimal control problem of train operation. *IEEE Trans. Automat. Contr.*, vol. 45, pp. 1257-1266.

Li, K. P.; Gao, Z. Y.; Ning, B. (2005): Modeling the railway traffic using cellular automata model. *Int. J. Mod. Phys. C*, vol. 16, pp. 921-932.

Liu, C.-S.; Atluri, S. N. (2011a): An iterative algorithm for solving a system of nonlinear algebraic equations, $\mathbf{F}(\mathbf{x}) = \mathbf{0}$, using the system of ODEs with an optimum α in $\dot{\mathbf{x}} = \lambda[\alpha\mathbf{F} + (1-\alpha)\mathbf{B}^{\mathrm{T}}\mathbf{F}]$; $B_{ij} = \partial F_i/\partial x_j$. *CMES: Computer Modeling in Engineering & Sciences*, vol. 73, pp. 395-431.

Liu, C.-S.; Atluri, S. N. (2012): A Globally Optimal Iterative Algorithm Using the Best Descent Vector $\dot{\mathbf{x}} = \lambda[\alpha_c\mathbf{F} + \mathbf{B}^{\mathrm{T}}\mathbf{F}]$, with the Critical Value α_c, for Solving a System of Nonlinear Algebraic Equations $\mathbf{F}(\mathbf{x}) = \mathbf{0}$. *CMES: Computer Modeling in Engineering & Sciences*, vol. 84, pp. 575-601.

Liu, C.-S.; Dai, H.-H.; Atluri, S. N. (2011a): A Further Study on Using $\dot{\mathbf{x}} =$

$\lambda[\alpha\mathbf{R} + \beta\mathbf{P}]$ ($\mathbf{P} = \mathbf{F} - \mathbf{R}(\mathbf{F} \cdot \mathbf{R})/\|\mathbf{R}\|^2$) and $\dot{\mathbf{x}} = \lambda[\alpha\mathbf{F} + \beta\mathbf{P}^*]$ ($\mathbf{P}^* = \mathbf{R} - \mathbf{F}(\mathbf{F} \cdot \mathbf{R})/\|\mathbf{F}\|^2$) in Iteratively Solving the Nonlinear System of Algebraic Equations $\mathbf{F}(\mathbf{x}) = \mathbf{0}$. *CMES: Computer Modeling in Engineering & Sciences*, vol. 81, pp. 195-227.

Liu, C.-S.; Dai, H.-H.; Atluri, S. N. (2011b): Iterative Solution of a System of Nonlinear Algebraic Equations $\mathbf{F}(\mathbf{x}) = 0$, Using $\dot{\mathbf{x}} = \lambda[\alpha\mathbf{R} + \beta\mathbf{P}]$ or $\dot{\mathbf{x}} = \lambda[\alpha\mathbf{F} + \beta\mathbf{P}^*]$ $\mathbf{R}$ is a Normal to a Hyper-Surface Function of $\mathbf{F}$, $\mathbf{P}$ Normal to $\mathbf{R}$, and $\mathbf{P}^*$ Normal to $\mathbf{F}$. *CMES: Computer Modeling in Engineering & Sciences*, vol. 81, pp. 335-362.

Liu, R.; Golovitcher, I. (2003): Energy-efficient operation of rail vehicles. *Transp. Res. A*, vol. 37, pp. 917-932.

Lu, Q.; Dessouky, M.; Leachman, R.C. (2004): Modeling train movements through complex rail networks. *ACM. Trans. Mod. Comput. Sim.*, Vol. 14, pp. 48-75.

Nagel, K.; Schreckenberg, M. (1992): Cellular automaton models for freeway traffic. *Phys. I*, vol. 2, pp. 2221–2229.

Ning, B.; Li, K. P.; Gao, Z. Y. (2005): Modeling fixed-block railway signaling system using cellular automata model. *Int. J. Mod. Phys. C*, vol. 16, pp. 1793-1801.

Ning, B.; Tang, T.; Dong, H.; Wen, D.; Liu, D.; Gao, S.; Wang, J. (2011): An introduction to parallel control and management for high-speed railway systems. *IEEE Trans. Intell. Transp. Syst.*, vol. 12, pp. 1473-1483.

Song, Q.; Song, Y.-D.; Tang, T.; Ning, B. (2011): Computationally inexpensive tracking control of high-speed trains with traction/braking saturation. *IEEE Trans. Intell. Transp. Syst.*, pp. 1116-1124.

Takeuchi, H.; Goodman, C. J.; Sone, S. (2003): Moving block signalling dynamics: performance measures and re-starting queued electric trains. *IEE Proc. - Electr. Power Appl.*, vol. 150, pp. 483-492.

Tang, T.; Li, K.-P. (2007): Traffic modeling for moving-block train control system. *Commun. Theor. Phys.*, vol. 47, pp. 601-606.

Wang, Y.; Hou, Z.; Li, X. (2008): A novel automatic train operation algorithm based on iterative learning control theory. *Proceedings of International Conference on Service Operations and Logistics, and Informatics*, pp. 1766-1770.

Xun, J.; Ning, B.; Li, K.-P. (2007): Network-based train-following model and study of train's delay propagation. *Acta Phys. Sin.*, vol. 56, pp. 5158-5164.

Xun, J.; Ning, B.; Li, K.-P. (2009): Station model for rail transit system using cellular automata. *Commun. Theor. Phys.*, vol. 51, pp. 595-599.

Yang, C.-D.; Sun, Y.-P. (2001): Mixed H_2/H_∞ cruise controller design for high

speed train. *Int. J. Control*, vol. 74, pp. 905-920.

Yasunobu, S.; Miyamoto, S.; Ihara, H. (1983): Fuzzy control for automatic train operation system. *Proceedings of 4th IFAC/IFIP/IFRS International Conference on Transportation Systems*, pp. 33-39.

Zhou, H.-L.; Gao, Z.-Y.; Li, K.-P. (2006): Cellular automaton model for moving-like block system and study of train's delay propagation. *Acta Phys. Sin.*, vol. 55, pp. 1706-1710.

Zhou, Y.; Mi, C. (2012): Modeling train movement for moving-block railway network using cellular automata. *CMES: Computer Modeling in Engineering & Sciences*, vol. 83, pp. 1-21.

Zhou, Y.; Mi, C.; Yang, X. (2012): The cellular automaton model of microscopic traffic simulation incorporating feedback control of various kinds of drivers. *CMES: Computer Modeling in Engineering & Sciences*, vol. 86, pp. 533-550.

Zhou, Y.; Wang, Y. (2011): Coordinated control among high-speed trains based on model predictive control. *Key Engineering Materials*, vol. 467-469, pp. 2143-2148.

Zhuan, X.; Xia, X. (2008): Speed regulation with measured output feedback in the control of heavy haul trains. *Automatica*, vol. 44, pp. 242-247.

Zhuan, X.; Xia, X. (2010): Fault-tolerant control of heavy-haul trains. *Veh. Syst. Dyn.*, vol. 48, pp. 705-735.